Algorithm for reconstruction of the ground surface reflection coefficients from the MODIS data taking into account the inhomogeneity of the ground surface

Mikhail V. Tarasenkov, Vladimir V. Belov, Anna V. Zimovaya, Marina V. Engel

V.E. Zuev Institute of Atmospheric Optics, Siberian Branch, Russian Academy of Sciences, Tomsk, Russia, TMV@iao.ru

Abstract. We consider an algorithm of atmospheric correction of satellite images for reconstruction the reflection coefficients of the ground surface in the visible and near-IR range. The algorithm accounts for the effect of inhomogeneity of the ground surface, adjacency effect, additional irradiance by reflected radiation, and polarization of radiation. The capabilities of this algorithm and MOD09 algorithm are compared using areas in Tomsk, Moscow, and Irkutsk regions of the Russian Federation as examples.

Keywords: remote sensing, MODIS, atmospheric correction, ground surface reflection coefficient, Monte Carlo method

1 Introduction

Satellite information on reflection coefficients of the ground surface has a wide applicability range. At the same time, the reflection coefficients are the result of indirect measurements and may have large errors. The smaller the algorithm-produced reconstruction error, the wider the satellite data applicability range is. As a consequence, atmospheric correction of satellite data is required in many situations. One of the directions in carrying out the atmospheric correction involves the use of the RTM algorithms. The approach is that a mathematical model of solar radiative transfer in the atmosphere-surface system and formation of received signal is constructed. Then, inverse problem is solved to determine the sought distribution of reflection coefficients over the ground surface.

In the general case, the intensity of received signal consists of: a) intensity of non-scattered radiation from the viewed surface area I_0, b) intensity of radiation scattered in the atmosphere and not having interacted with the ground surface I_{sun}, and c) intensity of radiation reflected by the neighboring areas on the ground surface and then being scattered in the atmosphere in the direction of receiver (adjacency effect) I_{surf}. In addition, ground surface is illuminated not only by direct and diffuse solar radiation, but also multiply (in the general case) surface-reflected radiation after being scattered in the atmosphere E_1, E_2, etc.

However, depending on the situations under consideration, a part of these quantities has a weak effect on the result of solving the inverse problem. Therefore, simplified models of radiative transfer in the atmosphere-surface system are constructed to speed up the solution in different algorithms of atmospheric correction. For instance, in one of the first works [1] the radiative transfer was accounted for in the approximation of single scattering of radiation and a homogeneous ground surface. In later works, such as in [2], a more adequate model of the optical radiative transfer was used; however, the atmospheric correction was carried out in the approximation of a homogeneous ground surface. In works similar to [3], the inverse problem was solved in two stages: (1) the reflection coefficient was determined in the approximation of a homogeneous surface, and (2) the adjacency effect was taken approximately into account. It was also assumed that the additional irradiance of the ground surface by reflected radiation is formed by a homogeneous surface. In work [4] the adjacency effect is taken rigorously into account, and an additional irradiance by reflected radiation is determined in the approximation of a homogeneous surface. In our works [5,6] we suggested an algorithm that accounts for the inhomogeneity of the ground surface in the formation of the adjacency effect and additional surface irradiance. This makes it possible to extend the algorithm of correction to include the situations with a high atmospheric turbidity and a complex non-uniform distribution of reflection coefficient over the ground surface.

Moreover, surface relief, surface non-Lambertianeity, polarization of radiation, and the effect of cloud fields on images of cloud-free areas may be significant factors in atmospheric correction. The problem on estimating the relief effect on the error of reconstruction the reflection properties of the ground surface was solved in [7,8]. The non-Lambertianeity was accounted for in [4,9,10]. We plan to consider these factors in our future works. Study of how cloud fields influence the cloud-free areas was initiated in our work [11]. The effect of polarization was estimated by

the authors of the works [12-14] for solving the direct problem of the solar radiative transfer in the atmosphere-surface system. Their estimates indicate that polarization may introduce an error up to 10% into the intensity of received radiation. In our works [15-16] it is shown that, in reconstruction the reflection coefficients of certain surfaces, the neglect of polarization may lead to absolute errors exceeding the value of reconstructed reflection coefficient. Therefore, the effect of polarization of radiation should be taken into consideration for areas covered, e.g., by weakly reflecting vegetation. Below, we will consider a modified algorithm of reconstruction the reflection coefficients, taking into account the polarization of radiation, and will verify it against MODIS images, as an example.

2 Algorithm of atmospheric correction with accounting for the polarization of radiation

The algorithm of correction was developed assuming that: the atmosphere is spherical and is divided into 32 homogeneous layers; the atmosphere is a scattering and absorbing medium; the ground surface is Lambertian; relief is disregarded; and the atmosphere partially polarizes radiation upon scattering.

This algorithm had been a basis for a software package, the block-diagram of which is presented in Figure 1.

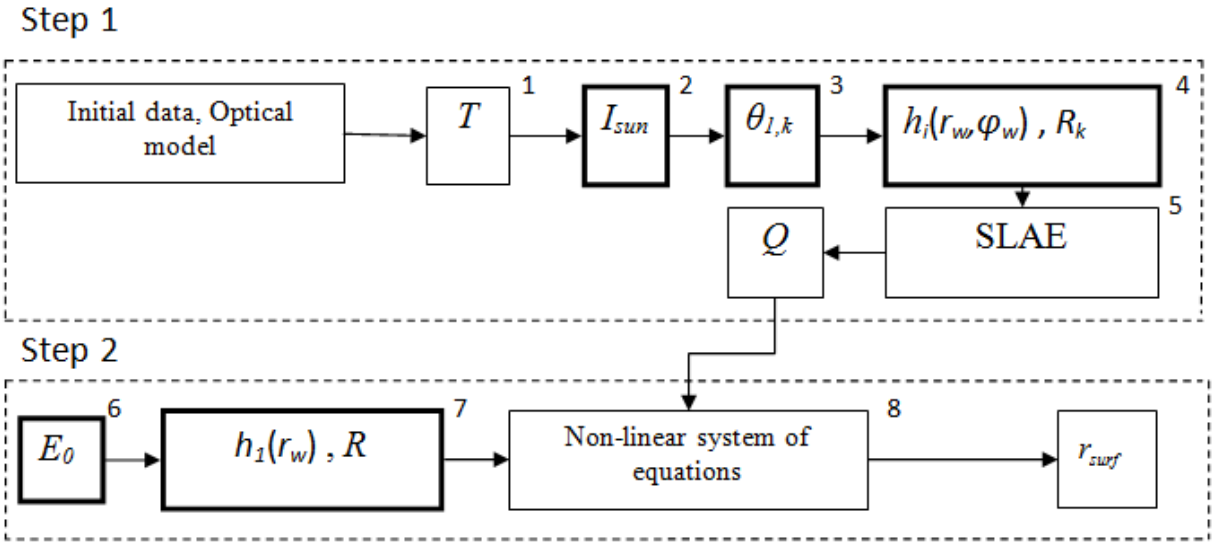

Figure 1. Block-diagram of software package. Blocks, in which algorithms of the Monte Carlo method are used, are highlighted by thick line.

The step-by-step procedure of atmospheric correction is as follows.

1) The direct transmission coefficient T_i of the path from the viewed pixel to receiving system is determined.

2) The Monte Carlo method is used to calculate the intensity of radiation I_{sun}, not having interacted with the ground surface, taking into account the polarization of radiation for 30 nodal directions. Based on these results, the approximate $I_{sun,I}$ values are determined from the formula:

$$I_{sun,i} = -\frac{B_i+\sqrt{B_i^2-4A_iC_{13}}}{2A_i\mu_{d,i}} \quad (1)$$

$$A_i = \begin{cases} C_{11}\mu_{d,i}^2 + C_{21}\left(\sqrt{1-\mu_{d,i}^2}\cos\varphi_i\right)^2 + C_{22}\mu_{d,i}\sqrt{1-\mu_{d,i}^2}\cos\varphi_i - \left(\sqrt{1-\mu_{d,i}^2}\sin\varphi_i\right)^2, \varphi_i \le 90^0 \\ C_{11}\mu_{d,i}^2 + C_{31}\left(\sqrt{1-\mu_{d,i}^2}\cos\varphi_i\right)^2 + C_{32}\mu_{d,i}\sqrt{1-\mu_{d,i}^2}\cos\varphi_i - \left(\sqrt{1-\mu_{d,i}^2}\sin\varphi_i\right)^2, \varphi_i > 90^0 \end{cases} \quad (2)$$

$$B_i = \begin{cases} C_{12}\mu_{d,i} + C_{23}\sqrt{1-\mu_{d,i}^2}\cos\varphi_i, \varphi_i \le 90^0 \\ C_{12}\mu_{d,i} + C_{33}\sqrt{1-\mu_{d,i}^2}\cos\varphi_i, \varphi_i > 90^0 \end{cases} \quad (3)$$

where $\mu_{d,i}$ is the cosine of the viewing zenith angle in observation of the *i*th pixel; φ_i is the azimuth between the directions toward Sun and toward receiver in the *i*th pixel; and C_{11}, C_{12}, C_{13}, C_{21}, C_{22}, C_{23}, C_{31}, C_{32}, and C_{33} are the approximation constants, determined by the least-squares method (LSM) from nodal I_{sun} values for a fixed θ_{sun}.

Algorithm of the I_{sun} calculation with accounting for polarization and its testing were described in [15,16].

3) The Monte Carlo method is used to calculate the nodal values of the integral of the point spread function (PSF) of the channel of formation of the adjacency effect I_{dif}. These results are used to determine the boundaries of isoplanar zones $\theta_{1,k}$, (regions on the ground surface within which the same PSF can be used with a specified error δ) according to the criterion:

$$\begin{cases} \mathrm{I}_{surf}(\mu_\mathrm{k}) = \mathrm{I}_{surf}(1) - \mathrm{A}(1-\mu_\mathrm{k})^\mathrm{N} \\ \mu_{\mathrm{k}+1} = 1 - \left[\frac{1}{\mathrm{A}}\left(\mathrm{I}_{surf}(1) - \frac{\mathrm{I}_{\mathrm{surf}}(\mu_\mathrm{k})}{1+\delta}\right)\right]^{1/\mathrm{N}} \end{cases} \quad (4)$$

$$\delta \equiv \frac{\mathrm{I}_{surf}(\mu_\mathrm{k}) - \mathrm{I}_{surf}(\mu_{\mathrm{k}+1})}{\mathrm{I}_{\mathrm{surf}}(\mu_{\mathrm{k}+1})} \quad (5)$$

$$\mathrm{I}_{surf}(\mu) \equiv \frac{T(\mu)}{\pi} + I_{dif}(\mu) = \frac{T(\mu)}{\pi} + \int_\mathrm{S} \mathrm{h}(\mu, \mathrm{r_w}, \varphi_\mathrm{w})\mathrm{d}s \quad (6)$$

where $\mu_k = cos\theta_{1,k}$ specifies the boundary between the *k*th and *k+1*st isoplanar zones; $T(\mu)$ is the direct transmission on the path from a point on the ground surface to receiving system for the cosine of angle of deviation from direction of nadir μ; $h(\mu, r_w, \varphi_w)$ is PSF of the channel of formation of adjacency effect; r_w is the surface distance from the center of the viewed pixel on the ground surface to a point on the ground surface; φ_w is the azimuth angle on the ground surface between the direction toward the projection of receiving system onto the ground surface and the direction toward a given point away from the pixel viewed; S is the entire area of the ground surface; δ is the maximum admissible error level in using PSF corresponding to μ_k, instead of PSF corresponding to μ_{k+1} (δ=0.05 was used in the calculations); and A, N are approximation constants determined using LSM.

4) The radius of the region of adjacency effect R_k is determined, outside of which the adjacency effect can be considered to be zero with a specified error δ_1. It can be shown that, in order for the condition:

$$1 \geq \min_i \frac{Q_i}{\overline{Q_i}} \geq \delta_1 \quad (7)$$

to be satisfied for an arbitrary inhomogeneous surface, where $\mathrm{Q_i} \equiv \mathrm{r_{surf,i}E_{sum,i}}$ is a certain exact value of the surface emissivity in the *i*th pixel; $\overline{\mathrm{Q_i}}$ is an approximate value of the emissivity, obtained assuming that no adjacency effect exists outside R_k; and δ_1 is a quantity, characterizing the maximal error due to the use of the radius of the adjacency effect ($\delta_1 = 0.95$ in our calculations), fulfillment of the condition is sufficient:

$$\mathrm{f_1(R_k)} \equiv \frac{\iint_{\mathrm{S(R_k)}} \mathrm{h}(\mu_\mathrm{k}, \mathrm{r_w}, \varphi_\mathrm{w})\mathrm{d}s}{\iint_\mathrm{S} \mathrm{h}(\mu_\mathrm{k}, \mathrm{r_w}, \varphi_\mathrm{w})\mathrm{d}s} \geq \delta_1 + (\delta_1 - 1)\frac{\frac{1}{\pi}\mathrm{T_k}}{\iint_\mathrm{S} \mathrm{h}(\mu_\mathrm{k}, \mathrm{r_w}, \varphi_\mathrm{w})\mathrm{d}s} \quad (8)$$

where R_k is the radius of the adjacency effect for the *k*th PSF, calculated for the angles (4); T_k is the direct transmission, corresponding to the boundary of the *k*th isoplanar zone; and $S(R_k)$ is the area on the ground surface within the radius R_k.

For MODIS channels considered below, for $0.1 \leq AOD_{0.55} \leq 5$, and for an arbitrary unknown distribution of reflection coefficients over the ground surface and different situations, in [6] upper estimates of R_k were obtained, for which the condition (8) is satisfied. The R_k value is within $3 \leq R_k \leq 40$ km, depending on λ, AOD, and positions of Sun and receiving system.

For each of k isoplanar zones, the Monte Carlo method is used to calculate PSF of the channel of formation of adjacency effect $\mathrm{h}(\mu_\mathrm{k}, \mathrm{r_w}, \varphi_\mathrm{w})$ within R_k.

5) The Seidel method is used to solve the system of linear algebraic equations (SLAE) for determining the distribution of emissivity of the ground surface Q_i:

$$\mathrm{I_{sum,i}} = \mathrm{I_{sun,i}} + \sum_{\mathrm{j}=1}^{\mathrm{N_i}} \mathrm{A_{i,j}Q_j} + \mathrm{A_{out,i}}\overline{\mathrm{Q_i}}\mathrm{i} = \overline{1,\mathrm{N}} \quad (9)$$

$$\mathrm{A_{i,j}} \approx \begin{cases} \frac{1}{\pi}\mathrm{T_i} + \mathrm{h}(\mu_{\mathrm{k_i}}, 0, 0)\mathrm{S_i}\,, \mathrm{i} = \mathrm{j} \\ \mathrm{h}(\mu_{\mathrm{k_i}}, \mathrm{r_{w,j}}, \varphi_{\mathrm{w,j}})\mathrm{S_j}\,, \mathrm{i} \neq \mathrm{j} \end{cases} \quad (10)$$

$$\mathrm{A_{out,i}} = \mathrm{I_{dif}}(\mu_{\mathrm{k_i}}) - \sum_{\mathrm{j}=1}^{\mathrm{N_i}} \mathrm{A_{i,j}} \quad (11)$$

$$\overline{\mathrm{Q_i}} = \frac{\mathrm{I_{sum,i}} - \mathrm{I_{sun,i}}}{\frac{1}{\pi}\mathrm{T_i} + \mathrm{I_{dif}}(\mu_{\mathrm{d,i}})} \quad (12)$$

where $I_{sum,i}$ is the intensity of total radiation received by satellite system; N is the number of pixels in the area under consideration; N_i is the number of pixels within the radius R_k around the *i*th pixel; μ_{k_i} is the boundary of the *k*th isoplanar zone into which the *i*th pixel falls; $\overline{Q_i}$ is the quantity that estimates approximately the surface emissivity outside the region under consideration; and S_i is the area of the *i*th pixel.

Solving the system of equations (9) for the entire area under consideration makes it possible to account for the inhomogeneity effect of the ground surface on the distribution of the surface emissivity.

6) The Monte Carlo method is used to calculate the irradiance of the ground surface without accounting for re-reflections E_0.

7) Radius is calculated for the region of formation of additional irradiance by singly reflected radiation R, outside of which the additional irradiance can be assumed to be zero. It can be shown that, in order for the condition:

$$1 \geq \min_i \frac{r_{surf,i}}{\widetilde{r_{surf,i}}} \geq \delta_1 \tag{13}$$

to be satisfied for an arbitrary inhomogeneous surface, where $r_{surf,i}$ is a certain reflection coefficient of the *i*th pixel; $\widetilde{r_{surf,i}}$ is an approximate value of the reflection coefficient, obtained in using the radius of the region of formation of additional irradiance; δ_2 is the quantity characterizing the maximal error due to the use of the radius of formation of additional irradiance ($\delta_2 = 0.95$ in our calculations), fulfillment of the condition is sufficient:

$$f_2(R) \equiv \frac{\iint_{S(R)} h_1(r_w)ds}{\gamma_1} \geq \frac{\delta_2}{\gamma_1}\left((\delta_2 - 1) + \delta_2\gamma_1\right) \tag{14}$$

$$\gamma_1 = \iint_S h_1(r_w)ds \tag{15}$$

where $h_1(r_w)$ is the value of PSF of channel of formation of additional irradiance.

For MODIS channels considered below, for $0.1 \leq AOD_{0.55} \leq 5$, and for different situations, in [6] we estimated R values, for which the condition (13) is satisfied. The R value is within $0 \leq R \leq 15$ km.

The Monte Carlo method is used to calculate PSF of channel where additional irradiance of the ground surface is formed by radiation reflected in the atmosphere-surface system $h_1(r_w)$ within the radius R.

8) The Newton method, with auxiliary SLAE solved iteratively by the Seidel method, is used to solve the nonlinear system of equations in r_{surf} of the form:

$$\frac{Q_i}{E_0} = r_{surf,i}\left(1 + \sum_{j=1}^{M_i} C_{i,j} r_{surf,j} + C_{out,i}\overline{r_{surf,i}} + \frac{\left(\overline{r_{surf,i}}\gamma_1\right)^2}{1-\overline{r_{surf,i}}\gamma_1}\right) \tag{16}$$

$$C_{i,j} \approx h_1(r_{w,ij})S_j \tag{17}$$

$$C_{out,i} = \gamma_1 - \sum_{j=1}^{M_i} C_{i,j} \tag{18}$$

$$\overline{r_{surf,i}} = \frac{\overline{Q_i}/E_0}{1+\gamma_1\overline{Q_i}/E_0} \tag{19}$$

where $r_{surf,i}$ is the reflection coefficient of the *i*th pixel of the image; $\overline{r_{surf,i}}$ is the reflection coefficient of the *i*th pixel, obtained in the approximation of a homogeneous ground surface; and M_i is the number of pixels within the radius R around the *i*th pixel.

Solving the nonlinear system (16) makes it possible to account for the effect of inhomogeneity of the ground surface on its irradiance. Analysis performed shows that, in the limiting situation out of those considered, with $AOD_{0.55}=5$, $r_{surf} \leq 0.4$, the error due to the use of (16) does not exceed 3%. At the same time, the neglect of the inhomogeneity effect of the ground surface in formation of additional irradiance in this situation leads to the errors within 19%. For a molecular atmosphere ($AOD_{0.55}=0$) and $r_{surf} \leq 0.4$ the error due to the use of (16) does not exceed 1%, and the error due to the use of homogeneous approximation (19) is 10.6%.

Analysis of convergence conditions for the systems of equations (9) and (16) in work [6] showed that the system (9) for any pixel size converges when $AOD \leq 1$, and with resolution at nadir of 1 km it converges when $AOD \leq 4$. System (16) converges for all situations considered in [6] ($0.1 \leq AOD_{0.55} \leq 5$).

3 Testing of algorithm.

To test the performance and to estimate the error of the algorithm of reconstruction the reflection coefficients with accounting for the polarization effect, we considered MODIS images for 5 channels: channel 1 centered at λ=0.649 μm, channel 2 at λ=0.860 μm, channel 3 at λ=0.469 μm, channel 4 at λ=0.555 μm, and channel 8 at λ=0.412 μm, with the spatial resolution of 1000 m. We considered three test regions 1) area in the south of Tomsk region (55.95^0 – 56.85^0N and 84.05^0 – 84.95^0E), 7 images from June 17, 2012 to June 23, 2012, 2) area in Moscow region (55.72^0-55.95^0N and 37.56^0-38.10^0E), 5 images from May 6, 2017 to May 7, 2017, and 3) area in Irkutsk region (51.42^0 -52.67^0N and 103.64^0 -105.47^0E), 4 images from June 20, 2017 to June 21, 2017. Results from our

algorithm with and without accounting for polarization were compared with those from MOD09 algorithm and those, obtained without atmospheric correction.

To estimate the errors of the algorithms, we considered test points at the centers of coniferous forest massifs. The errors of the algorithms were estimated as the difference between the reconstructed coefficients and measurements [17], presented in Table 1.

Table 1. Reflection coefficients of young needles of mature pine in summer period of the year, reproduced from [17].

λ, μm	0.412	0.469	0.555	0.645	0.860
$r_{surf,meas}(\lambda)$	0.021	0.026	0.050	0.038	0.310

As analysis showed, the reconstructed reflection coefficients for points at the centers of coniferous forest massifs in MODIS channels centered at λ=0.412, 0.469, 0.555, and 0.649 μm differ little from ground-based measurements presented in work [17] when aerosol content is small ($AOD_{0.55}\leq 0.1$). Therefore, for these channels and areas, the data from [17] can be used as reference values; and the differences from the data in [17] estimate approximately the errors of the algorithms. The reflection coefficients in the MODIS channel centered at λ= 0.860 μm differ from measurements in [17] markedly stronger because the reflection in this channel depends appreciably on the state (productivity) of vegetation. Therefore, data in [17] cannot be used as a reference for this channel in a number of situations.

AERONET data [18] on aerosol optical depth (AOD), particle size distribution, and complex refractive index were used as initial data for specifying the atmospheric model. Profiles of temperature and pressure from MODIS measurements [19] were additionally used. The $AOD_{0.55}$ values were in the range from 0.1 to 1.52 for the area in Tomsk region, from 0.04 to 0.07 for the area in Moscow region, and from 0.04 to 0.06 for the area in Irkutsk region. An example of reconstructed distributions of reflection coefficients over the ground surface is presented in Figure 2. Figure 3 presents an example of comparison of reflection coefficients of the ground surface, obtained using MOD09 algorithm and our algorithm with accounting for the polarization. From Figure 3 it can be seen that the results from the algorithms well agree for images with low atmospheric turbidity.

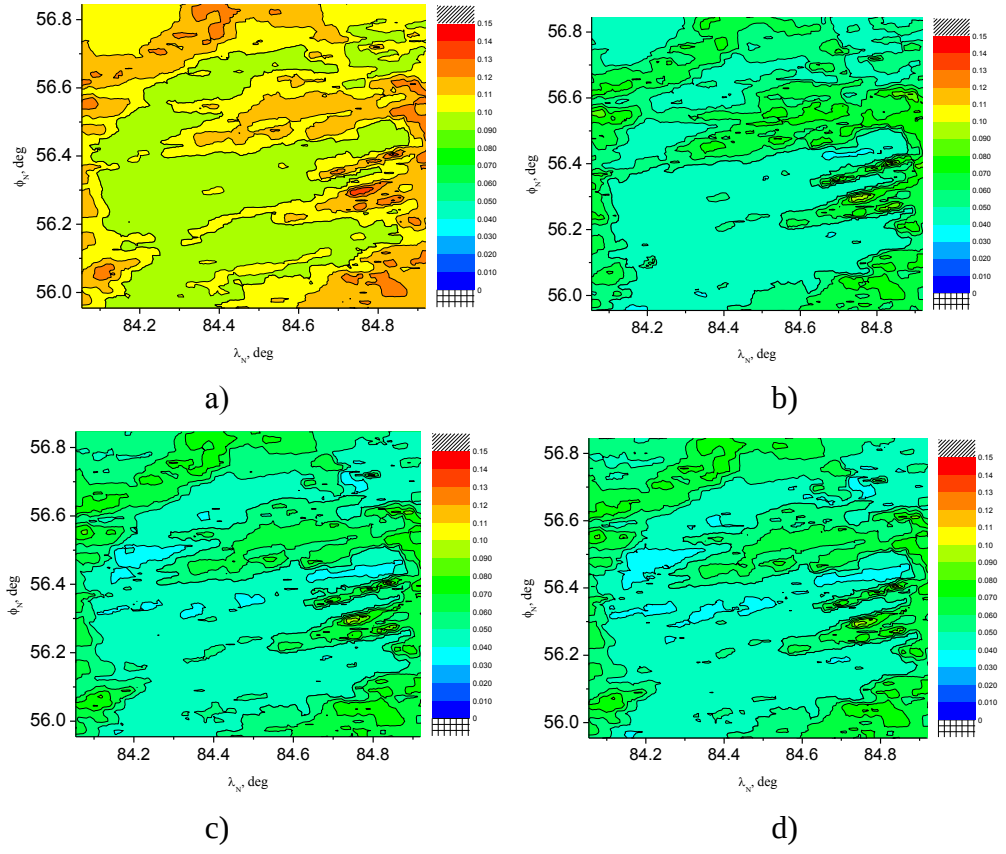

Figure 2. An example of reconstruction the reflection coefficient of the ground surface at λ=0.555 μm for an area in Tomsk region on June 22, 2012, at 07:45 UTC, onboard TERRA satellite. a) without correction, b) MOD09 algorithm, c) algorithm without accounting for polarization, and d) algorithm with accounting for polarization.

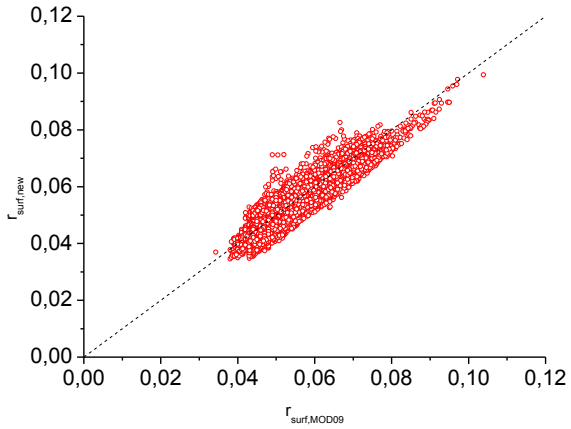

Figure 3. Comparison of reflection coefficients of the ground surface, obtained using MOD09 algorithm ($r_{surf,MOD09}$), with those, obtained using our algorithm with accounting for polarization ($r_{surf,new}$) for MODIS channel 4 (λ=0.555 μm) for an area in Tomsk region on June 22, 2012 at 07:45 UTC

The errors of these algorithms were estimated for 3 points (one point for each area): 1) a point on the territory of Tomsk State Nature Reserve (56.2^{0}N, 84.3^{0}E); 2) a point in Losiny Ostrov National Park (58.85^{0}N, 37.83^{0}E); and 3) a point in Krasny Yar State Nature Reserve (52.52^{0}N, 105.06^{0}E).

For each channel and each point, we determined the difference from reference value Δr_{surf}, averaged over these images. The average Δr_{surf} values thus obtained are presented in Table 2.

Table 2. Average difference Δr_{surf} from ground-based measurements [17].

Area no.	λ, μm	Δr_{surf}, algorithm without correction	Δr_{surf}, MOD09 algorithm	Δr_{surf}, algorithm without accounting for polarization	Δr_{surf}, algorithm with accounting for polarization
1	0.412	0.193	0.012	0.035	0.033
1	0.469	0.116	0.013	0.013	0.006
1	0.555	0.053	0.011	0.010	0.003
1	0.649	0.030	0.017	0.007	3.0E-5
1	0.860	0.031	0.021	0.034	0.027
2	0.412	0.164	0.017	0.018	0.018
2	0.469	0.094	0.009	0.009	0.008
2	0.555	0.035	0.012	0.011	0.011
2	0.649	0.027	0.010	0.010	0.010
2	0.860	0.155	0.157	0.155	0.156
3	0.412	0.173	0.014	0.008	0.011
3	0.469	0.098	0.010	0.009	0.008
3	0.555	0.047	0.012	0.010	0.010
3	0.649	0.023	0.011	0.008	0.010
3	0.860	0.035	0.036	0.036	0.030

Comparison of Δr_{surf} of our algorithm with Δr_{surf} of MOD09 algorithm for the point in Tomsk region shows that our algorithm with accounting for polarization for these test images shows markedly less differences from reference values for channels centered at λ=0.649, 0.469, and 0.555 μm and almost identical differences at λ=0.860 μm as compared to MOD09 NASA algorithm. However, the MOD09 values are closer to data in [17] at the wavelength of 0.412 μm.

For the test point in Moscow region, the reflection coefficients of the ground surface, reconstructed using algorithms considered here (except algorithm without atmospheric correction), deviate from the reference values by almost the same amount. The results for this point at λ=0.860 μm differ much stronger from data in [17] than those for the first point. This is probably because results in [17] strongly diverge from actual reflection coefficient in this channel and cannot be used as a reference for the situation, considered here.

Comparison of results for the test point in Irkutsk region shows that our algorithm with accounting for polarization for these images shows somewhat smaller differences from reference values at wavelengths 0.469, 0.555, and 0.412 μm than the MOD09 algorithm and almost identical differences at λ=0.860 and 0.649 μm.

4 Conclusions.

Comparison with MOD09 algorithm shows that our algorithm gives much smaller r_{surf} reconstruction errors than the MOD09 NASA algorithm at λ= 0.469, 0.555, and 0.649 μm, and gives an error of the same order of magnitude at λ= 0.860 μm. At λ= 0.412 μm, MOD09 algorithm reconstructs r_{surf} with a smaller error in some cases, our algorithm is more preferable in some other cases, and algorithms give errors of the same order of magnitude in the other cases.

References

[1] Otterman J., Fraser R.S. Adjacency effects on imaging by surface reflection and atmospheric scattering: cross radiance to zenith // Applied optics. 1979. Vol. 18, No. 16. P. 2852-2860.

[2] Vermote E.F., El Saleous N., Justice C.O., Kaufman Y.J., Privette J.L., Remer L., Roger J.C. and Tanre D. Atmospheric correction of visible to middle-infrared EOS-MODIS data over land surfaces: Background, operational algorithm and validation // Journal of geophysical research. 1997. Vol. 102, No. D14. P. 17,131-17,141.

[3] Vermote E.F., Vermeulen A. Atmospheric correction algorithm: spectral reflectances (MOD09). Algorithm Theoretical Background document, version 4.0. 1999. 107 p.

[4] Lyapustin A., Martonchik J., Wang Y., Laszlo I., Korkin S. Multiangle implementation of atmospheric correction (MAIAC): 3. Atmospheric correction // Remote Sensing of Environment. 2012. Vol. 127. P. 385-393.

[5] Tarasenkov M.V., Belov V.V. Software package for reconstructing reflective properties of the Earth's surface in the visible and UV ranges // Atmospheric and Oceanic Optics. 2015. Vol. 28. No. 1. P. 89-94.

[6] Tarasenkov M.V., Belov V.V., Engel M.V. Algorithm for reconstruction of the Earth surface reflectance from Modis satellite measurements in a turbid atmosphere // Proceedings of SPIE. 2018. V. 10833. CID: 10833 16 [10833-58].

[7] Gaofei Yin, Ainong Li, Shengbiao Wu, Weiliang Fan, Yelu Zeng, Kai Yan, Baodong Xu, Jing Li, Qinhuo Liu. PLC: A simple and semi-physical topographic correction method for vegetation canopies based on path length correction // Remote Sensing of Environment. 2018. Vol. 215. P. 184-198.

[8] Egorov V.A., Bartalev S.A. Radiometric correction for topography-induced distortions in land cover reflectance derived from satellite data // Sovremennye Problemy Distantsionnogo Zondirovaniya Zemli iz Kosmosa. 2016. Vol. 13. No. 5. P. 192-201.

[9] Breon FM., Vermote E. Correction of MODIS surface reflectance time series for BRDF effects // Remote Sensing of Environment. 2012. Vol. 125. P. 1-9.

[10] Lee T.Y., Kaufman Y.J. Non-Lambertian Effects on Remote-Sensing of Surface Reflectance and Vegetation Index // IEEE Transactions on Geoscience and Remote Sensing. 1986. Vol. 24, No. 5. P. 699-708.

[11] Tarasenkov M.V., Kirnos I.V., Belov V.V. Observation of the Earth's surface from the space through a gap in a cloud field // Atmospheric and oceanic optics. 2017. Vol. 30. No. 1. P. 39-43.

[12] Germogenova T.A. O vliyanii polyarizacii na raspredelenie intensivnosti rasseyannogo izlucheniya // Izv. AN SSSR. Ser.geofiz. 1962. Vol. 6. P. 854-856.

[13] Sushkevich T.A. Matematicheskie modeli perenosa izlucheniya. Moscow: BINON. Laboratoriya znanij, 2005.

[14] Nazaraliev M.A. Statisticheskoe modelirovanie radiacionnyh processov v atmosfere. Moscow: Nauka, 1990.

[15] Zimovaya A.V., Tarasenkov M.V., Belov V.V. Radiation polarization effect on the retrieval of the earth's surface reflection coefficient from satellite data in the visible wavelength range // Atmospheric and Oceanic Optics. 2018. Vol. 31, No. 2. P. 131-136.

[16] Zimovaya A.V., Tarasenkov M.V., Belov V.V. Effect of radiation polarization on reconstruction of the earth's surface reflection coefficient from satellite data in the visible wavelength range // Proceedings of SPIE. 2017. Vol. 10466. CID: 10466 10. [10466-54].

[17] Krinov E.L. Spektral'naya otrazhatel'naya sposobnost' prirodnyh obrazovanij. Leningrad. Izdatel'stvo Akademii Nauk SSSR, 1947.

[18] Aerosol Robotic Network (AERONET), http://aeronet.gsfc.nasa.gov

[19] https://lpdaac.usgs.gov/data_access